



HAL
open science

Copper(II)-containing chitosan-based non-toxic composites stimulate kefir grain biomass propagation: Combined in vitro and in vivo studies

Artem Dysin, Anatoly Kirichuk, Anton Egorov, Vladimir Kozyrev, Vasili Rubanik, Vasili Rubanik, Alexander Tskhovrebov, Dirk Schaumlöffel, Andreii Kritchenkov

► To cite this version:

Artem Dysin, Anatoly Kirichuk, Anton Egorov, Vladimir Kozyrev, Vasili Rubanik, et al.. Copper(II)-containing chitosan-based non-toxic composites stimulate kefir grain biomass propagation: Combined in vitro and in vivo studies. *Food Bioscience*, 2024, 58, pp.103741. 10.1016/j.fbio.2024.103741 . hal-04487721

HAL Id: hal-04487721

<https://univ-pau.hal.science/hal-04487721v1>

Submitted on 18 Nov 2024

HAL is a multi-disciplinary open access archive for the deposit and dissemination of scientific research documents, whether they are published or not. The documents may come from teaching and research institutions in France or abroad, or from public or private research centers.

L'archive ouverte pluridisciplinaire **HAL**, est destinée au dépôt et à la diffusion de documents scientifiques de niveau recherche, publiés ou non, émanant des établissements d'enseignement et de recherche français ou étrangers, des laboratoires publics ou privés.

**Copper(II)-Containing Chitosan-Based Non-Toxic Composites Stimulate Kefir Grain
Biomass Propagation: Combined *in vitro* and *in vivo* Studies**

Artem P. Dysin^a, Anatoly A. Kirichuk^a, Anton R. Egorov^a, Vladimir A. Kozyrev^a, Vasili V. Rubanik^b, Vasili V. Rubanik-Jr^b, Alexander G. Tskhovrebov^a, Dirk Schaumlöffel^{a,c}, and Andreii S. Kritchenkov^{a,b*}

^a *RUDN University, 6 Miklukho-Maklaya St, Moscow, 117198, Russian Federation*

^b *Institute of Technical Acoustics NAS of Belarus, Ludnikova Prosp. 13, Vitebsk, 210009, Republic of Belarus*

^c *CNRS, Université de Pau et des Pays de l'Adour, E2S UPPA, Institut des Sciences Analytiques et de Physico-Chimie pour l'Environnement et les Matériaux (IPREM), UMR 5254, 64000 Pau, France*

* Corresponding author at Peoples' Friendship University of Russia (RUDN University), Miklukho-Maklaya str. 6, Moscow, 117198, Russian Federation.

E-mail address: kritchenkov-as@rudn.ru (Andreii S. Kritchenkov)

Tel.: +79819365895

Fax: +74959540336

Abstract

In this study, we designed innovative Cu(II)/Chitosan-based systems: (1) the simplest Cu(II)/Chitosan blended composites, (2) the hyaluronate-covered, (3) cholesterol containing, (4) the simplest succinated, and (5) the hyaluronate-covered succinated ones. Blending of Cu²⁺ and succinated chitosan (4) or succinated chitosan covered by hyaluronate (5) stimulated kefir grain propagation. The maximum of the stimulation effect was observed in the case of succinated hyaluronate covered Cu(II)/Chitosan-based systems (5), which were identified as the undisputed leaders. The observed phenomenon was explained by symbiotic action of Cu(II) cations and polymeric matrices. We also evaluated the *in vitro* and *in vivo* toxicity of the composites. The most *in vitro* toxic were found to be cholesterol containing systems (3), while hyaluronate-covered succinated composites (5) demonstrated the minimum toxic effect toward living cells HEK-293. The leading composites also demonstrated low *in vivo* acute and subacute toxicity which allowed us to refer them to the IV class of hazard (low-toxic substances). Due to their low toxicity and high ability to stimulate the growth of kefir grain biomass, the leading composites are of interest for further research, for example, in the food industry.

1. Introduction

Chitosan is a natural eco-friendly amino polysaccharide which is characterized by biodegradability and biocompatibility (Lari et al., 2011; Pooladi and Bazargan-Lari, 2023). Interaction of chitosan with copper(II) ions proceeds along the complex formation pathway (Kritchenkov et al., 2013; Mekahlia and Bouzid, 2009; Varlamov et al., 2020) and results in a number of materials with attractive biological properties which combine those of natural non-toxic biopolymer chitosan and biologically active Cu^{2+} cation. Among these functional materials are scaffolds for regenerative medicine (Zhao et al., 2022), aerogels (Tang et al., 2022), hydrogels for photodynamic cancer chemotherapy (Qian et al., 2022), a large variety antibacterial system (Goy et al., 2009; Kritchenkov et al., 2020b; Kritchenkov et al., 2020c), and even copper/chitosan nanoparticles, which elicit tolerance against hyperosmotic stress and salinity in wheat (Farooq et al., 2022).

The search for new suitable bioelement-based compounds that can increase the growth of producing microorganisms biomass is one of the most challenging tasks of bioinorganic chemistry, biotechnology, and biochemistry. Among a number of inorganic ions promoting bacterial growth, copper deserved special attention as a bioactive microbial supplement. At high concentrations, Cu^{2+} acts as an antibacterial agent, while at low concentrations, copper(II) increases kefir grain biomass growth, yogurt starter, and a number of other valuable microorganisms and their symbioses (Han et al., 2012). The same can be said about chitosan. On the one hand, chitosan exhibits antimicrobial properties against a number of pathogenic bacteria and fungi (Goy et al., 2009; Qin et al., 2020), and on the other hand, chitosan can stimulate the growth of a number of useful producing microorganisms in biotechnology (Gandra et al., 2018; Hosseinejad and Jafari, 2016; Liu et al., 2018; Sahariah and Másson, 2017; Shih et al., 2019).

Although the individual effect of the Cu^{2+} or chitosan on producing microorganisms growth is partly known, examples of the effect of Cu^{2+} /chitosan systems on producing microorganisms

are not presented in the literature. The effect of Cu^{2+} /chitosan system can strongly depend on the molecular weight of chitosan, as well as on the variant of its chemical modification.

In the present study, we elaborated a scope of Cu^{2+} /chitosan systems differing in the parameters mentioned above (see **Figure 1**). These include, firstly, Cu^{2+} /chitosan systems, which contain copper(II) sulfate (1–3) or copper(II) acetate (4–6) as the source of copper ions.

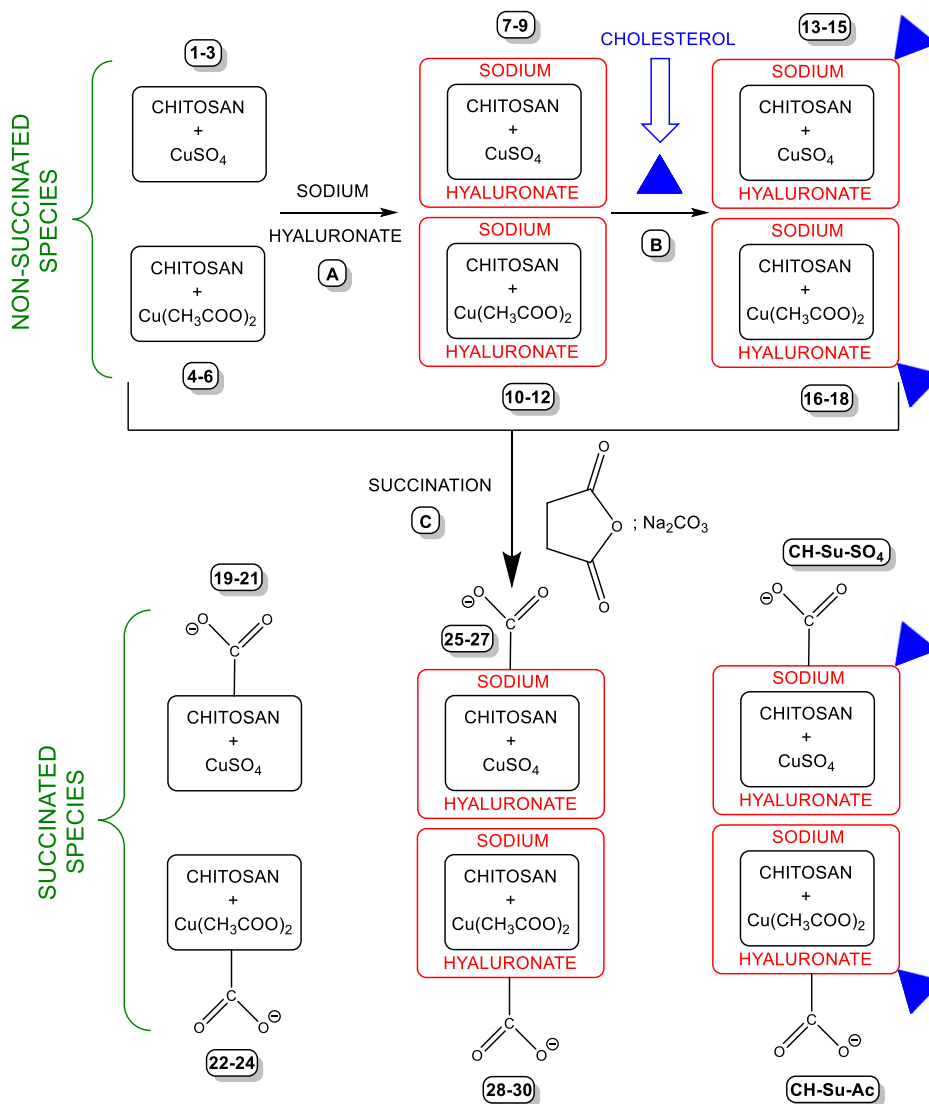


Figure 1. The elaborated Cu^{2+} /chitosan systems.

Coating positively charged particles of M^{n+} /chitosan system with a polyanionic layer can significantly reduce the toxicity of the starting particles and give them new types of biological activity (Mallik et al., 2020). The formation of a polyelectrolyte complex between positively

charged **1–3** or **4–6** and negatively charged sodium hyaluronate leads to the formation of **7–9** and **10–12**, respectively. Conjugation of many micro- and nanoparticles with cholesterol changes the hydrophilic-lipophilic balance, leads to better interaction with the membrane cell, and often can result in enhanced or unexpected biological effects. Conjugation of **7–9** and **10–12** with cholesterol allows one to obtain new systems **13–15** and **16–18**.

Chitosan-based systems succination is another important way to reduce toxicity and impart new types of biological activities (antiaggregant, anticoagulant, antioxidant, thrombolytic, etc.) (Bashir et al., 2015). Systems **1–3** and **4–6**, **7–9** and **10–12**, and **13–15** and **16–18** were treated with succinic anhydride to form the corresponding succinated systems **19–21** and **22–24**, **25–27** and **28–30**, and **CH–Su–SO₄** and **CH–Su–Ac**.

Each of the systems mentioned in **Figure 1** was prepared using either copper(II) sulfate or copper(II) acetate as a source of Cu²⁺, in order to determine the effect of the counterion (SO₄²⁻ or AcO⁻) on the structure of the formed Cu²⁺/chitosan systems and their biological effect. In addition, to identify the effect of molecular weight on biological properties, each system presented in **Figure 1** was obtained from low molecular weight (12 kDa, CH_I), medium molecular weight (300 kDa, CH_{II}) and high molecular weight (500 kDa, CH_{III}) chitosan.

The preparation, characterization, and study of the effect of the resulting Cu²⁺/chitosan systems on kefir grain biomass growth are discussed in the sections that follow below.

2. Materials and methods

Chitosan of viscosity-average molecular weights 12, 200 and 500 kDa and degree of acetylation 10 % were from Bioprogress (Moscow, Russia). Copper(II) sulfate pentahydrate, copper(II) acetate dihydrate, succinic anhydride were also purchased from Sigma Aldrich. Other chemicals and solvents were also from commercial sources and used as received without any further purification.

Particle size measurements were determined by dynamic light scattering using a thermally stabilized semiconductor laser with a wavelength of 638 nm on a Photocor Compact-Z particle size analyzer at 25 °C.

Zeta-potential was measured by electrophoretic light scattering on a Photocor Compact-Z device.

IR spectra of were recorded on a Shimadzu IRPrestige 21 Fourier transform IR spectrometer equipped with an MCT detector using a Miracle ATR unit manufactured by Pike.

Differential thermal thermogravimetric analysis was performed on an SDT Q600 thermal analyzer (TA Instruments, USA) with heating rate 10 deg/min.

X-ray analysis of the samples was carried out on a Dron-7 X-ray diffractometer. 2θ angle interval from 7° to 40° with scanning step $\Delta 2\theta = 0.02^\circ$ and exposure of 7 s per point. Cu K_{α} radiation (Ni filter) was used, which was subsequently decomposed into $K_{\alpha 1}$ and $K_{\alpha 2}$ components during processing of the spectra.

Inductively coupled plasma-atomic emission spectroscopy measurements were performed with a Leeman ICP-AES Prodigy XP spectrometer.

2.1. Preparation and characterization of Cu^{2+} -containig composites

Composites **1–6**. 0.150 g of chitosan was added to 150 ml of 1% CH_3COOH (pH ca. 3.6) and stirred for 1 hour to obtain transparent solution. A solution 0.150 g of copper(II) sulfate pentahydrate (for **1–3**) or copper(II) acetate dihydrate (for **4–6**) in distilled water (150 ml) was dropwise added to the vigorously stirred chitosan solution. The obtained composites were lyophilized.

Composites **7–12**. Any of composites **1–6** (0.300 g) was dispersed in 150 ml of distilled water and stirred for 1 hour. Sodium hyaluronate solution (0.150 g per 150 ml of distilled water) was dropwise added to the vigorously stirred to **1–6** suspension and intensively stirred for 5 minutes. The resultant composites were lyophilized.

Composites **13–18**. A solution of cholesterol-conjugated chitosan with degree of substitution 0.3 was dissolved in 1 % acetic acid (1 mg/ml) was added to a solution of copper(II) sulfate pentahydrate or copper(II) acetate dihydrate (1 mg/ml) and stirred for 1 hour. The resulting composites were freeze-dried.

Succinated composites. 0.300 g of succinic anhydride was dissolved in 10 ml and 0.100 g of any of **1–18** was added; resultant suspension was vigorously stirred overnight at 50 °C. The reaction mixture was centrifuged, and the precipitate was washed with ethyl acetate, water, 5 % sodium bicarbonate solution and again water. The washed precipitate was dispersed in water (15 ml), frozen and lyophilized.

The mentioned mass ratios are essential for generation of the Cu²⁺-containing systems with described characteristics.

2.2. *Kefir experiment*

Experiments to study the growth dynamics of kefir fungus biomass were carried out using as a nutrient medium fresh skimmed cow's milk with a brief ultra-high temperature treatment (ultra-pasteurized) with the following chemical composition: proteins 3.3%, fats 0.1%, carbohydrates 5.2%, Ca²⁺ 0.12%.

Inactivated kefir grains were inoculated into milk and kept at 25 °C for 24 hours. Kefir grains were separated from fermented milk by filtration through a glass sieve and washed with purified water. This procedure was repeated 6 times, after which the grains were considered active.

Milk fermentation experiments were carried out as follows. 100 ml of milk was heated in a water bath to 25 °C with occasional stirring. 5 minutes after the steady achievement of the set temperature, the activated grains of kefir fungus were placed in milk. The resulting mass was stirred under thermostating conditions at a constant speed of rotation of the blade of a mechanical stirrer 90 rpm for 24 h, periodically measuring the pH of the medium. To study the growth dynamics of kefir fungus biomass, kefir grains were filtered through a glass sieve from the

fermented milk mass, washed with purified water, thoroughly blotted with sheets of filter paper to dry it from excess moisture, and weighed on technochemical scales. Three experiments were carried out in parallel, and the spread of their reproducibility was within $\pm 5\%$. To study the effect of additives on the growth of kefir fungus biomass, the additive was placed in skimmed cow's milk, after which a fermentation experiment was carried out as described above. The initial concentration of kefir grains was 8%.

2.3. In vitro and in vivo toxicity studies

The *in vitro* toxicity was estimated by the MTT test. Solutions or nanosuspensions of the tested samples were prepared by serial dilution in alpha-MEM culture medium. A 0.1 mL volume of each of nanosuspension was added to a confluent monolayer of cells cultured in a 96-well plate. Cells were incubated for 24 h at 37 °C in an atmosphere containing 5% CO₂. The cells were washed twice with PBS and then 0.1 mL of 3-(4,5-dimethylthiazolyl)- 2,5-diphenyltetrazolium bromide (MTT, 0.5 µg/mL) in PBS was added and the mixture was incubated for 4 h. The supernatant was then replaced with 0.1 mL of 96% ethanol, and the absorbance was measured at 535 nm.

The *in vivo* toxicity in white rats was studied as described elsewhere (Sahm, 1991). Animal procedures were compliant with the Ethics Committee and followed the recommendations of European Directive 2010/63/EU of 22 September 2010.

2.4. Statistical analysis

The statistical significance of differences between the samples was determined by one-way analysis of variance (ANOVA) using JMP 5.0.1 software (SAS Campus Drive, Cary, NC). Mean values, where appropriate, were compared by Student's *t*-test at a significance level $p < 0.05$.

3. Results and discussion

3.1. Preparation and characterization of Cu²⁺/chitosan systems

3.1.1. Preparation of Cu²⁺/chitosan systems

The prepared samples are presented in **Table 1**. Samples **1–6** are the simplest in their chemical composition and were obtained by coordination of NH₂ and OH groups of chitosan to Cu(II) center as a result of mixing of chitosan (CS) in 1% acetic acid and aqueous solution of CuSO₄ (samples **1–3**) or Cu(CH₃COO)₂ (samples **4–6**). Samples **7–12** were obtained by gentle coating of the corresponding highly cationic samples **1–6** by polyanion of sodium hyaluronate (NaHA), see **Scheme 1, route a**. Samples **13–18** were prepared by addition CuSO₄ (samples **13–15**) or Cu(CH₃COO)₂ (samples **16–18**) to cholesterol-chitosan derivative followed by coating with sodium hyaluronate layer. Thus, **13–18** differ from **7–12** by the presence of the cholesterol substituent (**Scheme 1, route b**). Introduction of hydrophobic cholesterol moiety into the chitosan macromolecule was performed to increase the interaction of **13–18** with microbial cell (Cammarata et al., 2015; Williams and Ibrahim, 1981).

The succinated samples **19–30** were prepared by succination of the corresponding non-succinated samples (**Scheme 1, route c**) according to the standard procedure (Bashir et al., 2015). Thus, succination of **1–6** gave rise **19–24** while succination of **7–12** afforded **25–30**. Succination of **13–18** has not been performed these samples, as it turned out, are characterized by the worst biological properties (see section 3.3).

Table 1. Characteristics of the prepared Cu(II)-based systems

| Composition of the sample | N ^o | Size, nm | Zeta-potential, mV | Cu ²⁺ content, % | Cell viability, % |
|---|----------------|----------|--------------------|-----------------------------|-------------------|
| Chitosan | - | - | - | - | 98 |
| Copper(II) acetate | - | - | - | - | 28 |
| <i>Non-succinated species</i> | | | | | |
| CH _I +Cu(II) sulfate | 1 | 307 | 13.98±0.32 | 17.4 | 72 |
| CH _{II} +Cu(II) sulfate | 2 | 266 | 14.16±0.13 | 18.1 | 74 |
| CH _{III} +Cu(II) sulfate | 3 | 286 | 14.07±0.14 | 17.7 | 74 |
| CH _I +Cu(II) acetate | 4 | - | - | 13.3 | 83 |
| CH _{II} +Cu(II) acetate | 5 | - | - | 13.8 | 84 |
| CH _{III} +Cu(II) acetate | 6 | - | - | 13.6 | 84 |
| CH _I +Cu(II) sulfate+hyaluronate | 7 | 329 | 7.08±0.10 | 13.2 | 85 |
| CH _{II} +Cu(II) sulfate+hyaluronate | 8 | 271 | 7.03±1.12 | 13.0 | 85 |
| CH _{III} +Cu(II) sulfate+hyaluronate | 9 | 288 | 7.37±0.07 | 13.0 | 86 |

| | | | | | |
|---|----|-----|------------|------|----|
| CH _I +Cu(II) acetate+hyaluronate | 10 | - | - | 8.3 | 81 |
| CH _{II} +Cu(II) acetate+hyaluronate | 11 | - | - | 8.5 | 80 |
| CH _{III} +Cu(II) | 12 | - | - | 8.7 | 83 |
| CH _I +Cu(II) sulfate+cholesterol | 13 | 99 | 8.22±0.17 | 15.7 | 64 |
| CH _{II} +Cu(II) sulfate+cholesterol | 14 | 108 | 8.55±0.15 | 15.7 | 65 |
| CH _{III} +Cu(II) sulfate+cholesterol | 15 | 93 | 8.37±0.21 | 15.5 | 65 |
| CH _I +Cu(II) acetate+cholesterol | 16 | - | - | 10.9 | 63 |
| CH _{II} +Cu(II) acetate+cholesterol | 17 | - | - | 10.4 | 65 |
| CH _{III} +Cu(II) acetate+cholesterol | 18 | - | - | 10.6 | 63 |
| <i>Succinated species</i> | | | | | |
| CH _I +Cu(II) sulfate | 19 | 287 | -4.14±0.22 | 10.1 | 86 |
| CH _{II} +Cu(II) sulfate | 20 | 271 | -4.62±0.10 | 10.0 | 86 |
| CH _{III} +Cu(II) sulfate | 21 | 290 | -4.23±0.17 | 10.0 | 88 |
| CH _I +Cu(II) acetate | 22 | - | - | 7.4 | 92 |
| CH _{II} +Cu(II) acetate | 23 | - | - | 7.6 | 90 |
| CH _{III} +Cu(II) acetate | 24 | - | - | 7.7 | 90 |
| CH _I +Cu(II) sulfate+hyaluronate | 25 | 315 | - | 8.3 | 96 |
| CH _{II} +Cu(II) sulfate+hyaluronate | 26 | 276 | - | 8.4 | 96 |
| CH _{III} +Cu(II) sulfate+hyaluronate | 27 | 283 | - | 8.2 | 95 |
| CH _I +Cu(II) acetate+hyaluronate | 28 | 315 | - | 5.6 | 97 |
| CH _{II} +Cu(II) acetate+hyaluronate | 29 | 284 | - | 5.8 | 95 |
| CH _{III} +Cu(II) | 30 | 303 | -20.74±0.1 | 5.8 | 96 |

3.1.2. Physical forms and characterization of the obtained samples

For all non-succinated species, the samples obtained using CuSO₄ as a source of Cu²⁺, were of submicron level (1–3, 7–9, and 13–15, **Table 1**). In chitosan chemistry, particles of such sizes are commonly referred to nanoparticles (Yanat and Schroën, 2021). The simplest nanoparticles 1–3 as well as sodium hyaluronate covered nanoparticles 7–9 were characterized by their hydrodynamic diameter ca. 300 nm. At the same moment, cholesterol-derived nanoparticles 13–15 were of ca. 100 nm in their hydrodynamic diameter. In contrast with CuSO₄, the samples prepared using Cu(CH₃COO)₂ as a copper(II) source, are not prone to the formation of nanoparticles.

In the case of succinated samples (19–30, **Table 1**), only 22–24 do not form nanoparticles. 19–21 were of the smallest size among succinated nanoparticles (ca. 200 nm), while 25–30 had hydrodynamic diameter of ca. 600 nm. The example of SEM image of the prepared nanoparticles is presented in **Figure 2**.

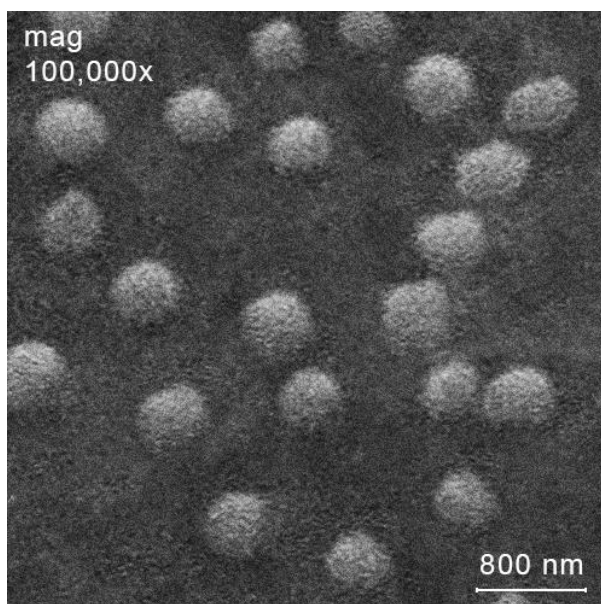


Figure 2. SEM image of CH_{III}+Cu(II) acetate+hyaluronate.

ζ -Potential of nanoparticles is extremely important physical parameter affecting their stability and biological properties. The simplest nanoparticles **1–3** had ζ -potential ca. +14 mV. Treatment of **1–3** by polyanion sodium alginate expectedly reduced the potential of the resulting nanoparticles **7–9** to ca. 7 mV. ζ -Potential of cholesterol-containing nanoparticles **13–15** was ca. 8 mV. Succination of nanoparticles **1–12** dramatically reduced the ζ -potential of resultant **19–21** and **25–30** to negative values (up to 18–21 mV). Moreover, it should be noted that neither the size nor the ζ -potential of the obtained nanoparticles practically depended on the molecular weight of the chitosan used (see **Table 1**).

The copper(II) content in the samples was measured by X-ray fluorescence analysis and it is presented in **Table 1**. Degree of succination of the succinated species was determined via C,H,N elemental analysis (see (Skorik et al., 2017)) and was ca. 20 %.

3.1.3. X-Ray diffraction study

In the biological section of this study, we will clearly see that the biological properties of prepared samples **1–30** depend not only on the size and zeta potential of the particles, but also on their microstructure, which can be characterized using X-Ray diffraction study.

In addition to the main expressed chitosan peak at ca. $17\text{--}27^\circ 2\theta$, the diffractograms of samples **1–12** (for X-Ray diffraction, see **Figure 3**) also display intense crystalline peaks at 13° , 14.25° , 15° , and $16.5^\circ 2\theta$, which correspond to hydrated copper(II) acetate. This is a strong evidence that not all copper(II) ions entered into a coordination interaction with chitosan, some of them are in the composition of copper(II) acetate crystals. It is noteworthy that when copper(II) sulfate is used for the synthesis of nanoparticles, the diffraction patterns still show a peak corresponding to copper(II) acetate. This fact is probably due to the use of a large amount of CH_3COOH as the chitosan solvent and the lower solubility of copper(II) acetate in comparison with copper(II) sulfate. The X-Ray diffraction patterns of **7–12** exhibit demonstrates also additional peaks due to sodium hyaluronate (9.8° , $10.2^\circ 2\theta$).

In contrast to the above, the X-ray diffraction patterns of cholesterol-containing samples **13–15** prepared from copper(II) sulfate display CuSO_4 crystalline peaks, while $\text{Cu}(\text{CH}_3\text{COO})_2$ -based cholesterol-containing species **16–18** quite naturally contain crystalline copper(II) acetate.

Remarkably, a higher content of crystalline copper(II) salt (sulfate or acetate, depending on the situation) is characteristic of cholesterol-containing samples **13–18** than cholesterol-free ones **1–12**. Thus, cholesterol-containing samples coordinate copper(II) to a lesser extent and, as a result, the largest fraction of the copper(II) salt in composition **13–18** is contained in the crystalline state. This fact is explained by the increased hydrophobicity of cholesterol-containing samples in comparison with cholesterol-free ones.

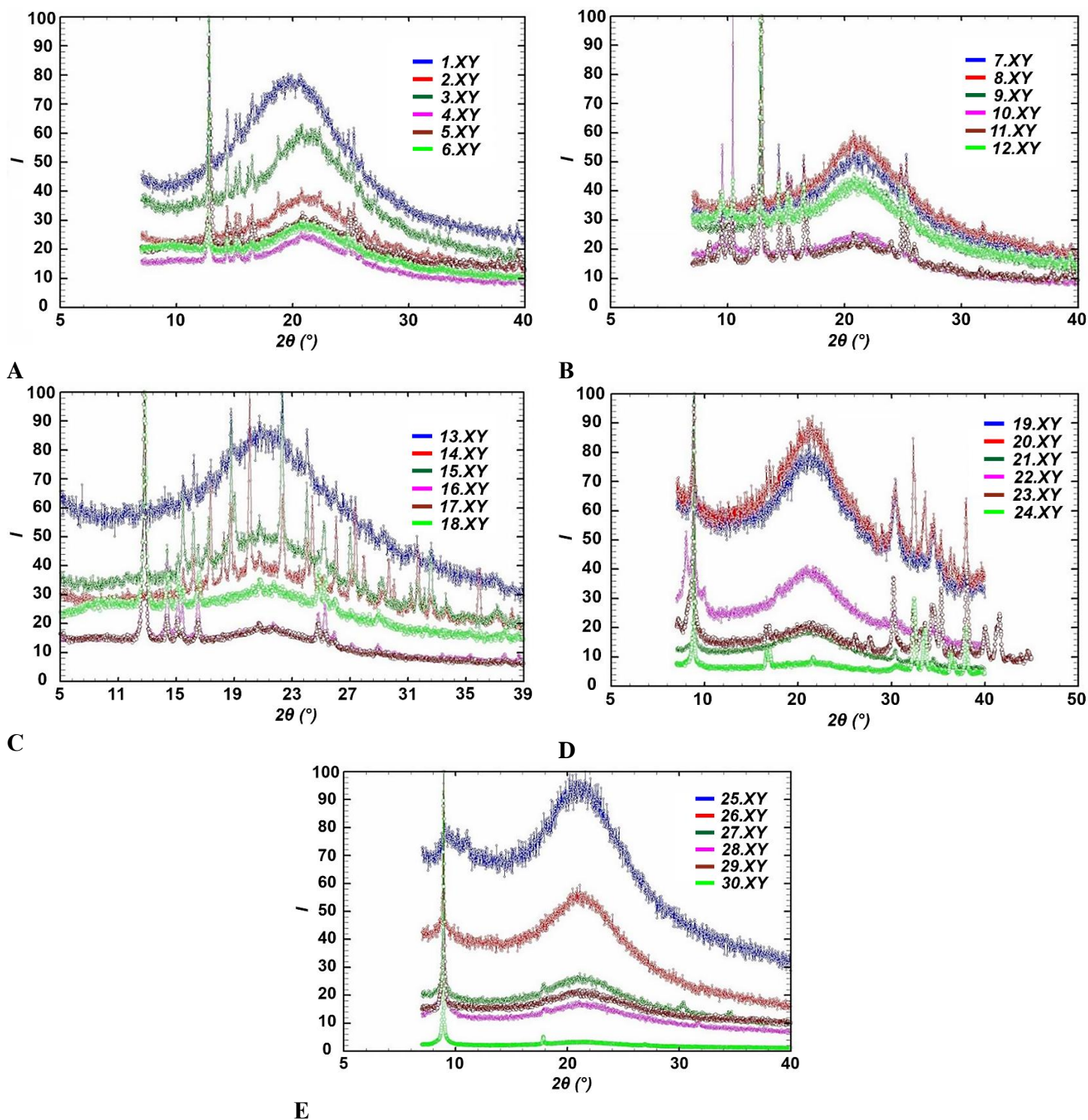


Figure 3. X-Ray diffractograms of 1–6 (A), 7–12 (B), 13–18 (C), 19–24 (D), 25–30 (E), normalized to the main peak.

In succinated samples 25–30, all Cu(II) ions are coordinated to NH₂ and OH groups of chitosan, and this is in agreement with absence of both copper(II) sulfate and copper(II) acetate

peaks in diffractograms of **25–30**. According to X-Ray analysis, **25–30** entirely composed of amorphous phase.

Thus, samples **1–30** are characterized by existence either in the physical form of nano-level particles (**1–3, 7–9, 13–15, 19–21, 25–30**) or in the coarser powdered form (**4–6, 10–12, 16–18, 22–24**). Moreover, among **1–30**, **25–30** consist only from polymeric amorphous phase, while the additional presence of crystalline phase due to copper(II) salts is characteristic for samples **1–24**.

3.1.4. FTIR characterization

The infrared spectra of all obtained copper-containing chitosan-based composites were compared with those of the starting polymers and copper(II) salts (see **Figures S1-S7**, Supplementary Materials). The spectra of **1–12** (**Figure S3** and **S4**) show the decrease in width and intensity of OH and NH stretching vibrations bands, which is due to the weakening of the hydrogen bonds caused by the coordination of the hydroxy and amino functionalities to Cu²⁺ center. Primary amino group banding vibrations band is shifted from 1655 to 1605 cm⁻¹ due to the binding of NH₂ group to the metal ion. The spectra of **1–18** (**Figure S3-S5**) naturally display the intense bands of the starting copper(II) salts, which is totally in agreement with the X-Ray diffraction analysis data. Succinated composites **19–30** exhibit intense bands at 1630 cm⁻¹ in their IR spectra (**Figure S6** and **S7**). This band is due to stretching vibrations of C=O moiety of amide functionality originated as a result of the succination.

3.2. Biological studies

3.2.1. Kefir grains experiments

At the first stage of the biological experiments, we determined the optimal initial concentration of kefir grains in order to use this concentration in the subsequent stages of the experimental work. The optimal concentration of kefir grains is the concentration which results in

(i) the minimum pH value of the kefir fermentation liquid and (ii) the maximum value of the kefir biomass growth. The determination of the optimal concentration of kefir grains was carried out without the use of any additives that stimulate the growth of the biomass.

The initial pH value of the kefir fermentation liquid was 6.70, which corresponds to the norm [9]. 24 hours after the start of the experiment, the pH value decreased to 4.10, 4.00, 3.95, 3.85, and 3.70 at an initial concentration of kefir grains of 2 %, 4 %, 6 %, 8 %, and 10 %, respectively (**Figure 4**). The observed decrease in pH can be explained by an increase in the number of acid-producing microorganisms. This assumption was confirmed in the following experiment. We studied the change in the biomass of kefir grains over 24 hours at various initial concentrations of kefir grains (2 %, 4 %, 6 %, 8 % and 10%). Indeed, the biomass growth was 7 %, 13 %, 21 %, 30 %, and 19 %, respectively (**Figure 5**). Thus, both the decrease in pH and the increase in biomass reach their apogee when using an initial concentration of kefir grains of 8 % and this concentration was chosen as the optimal one.

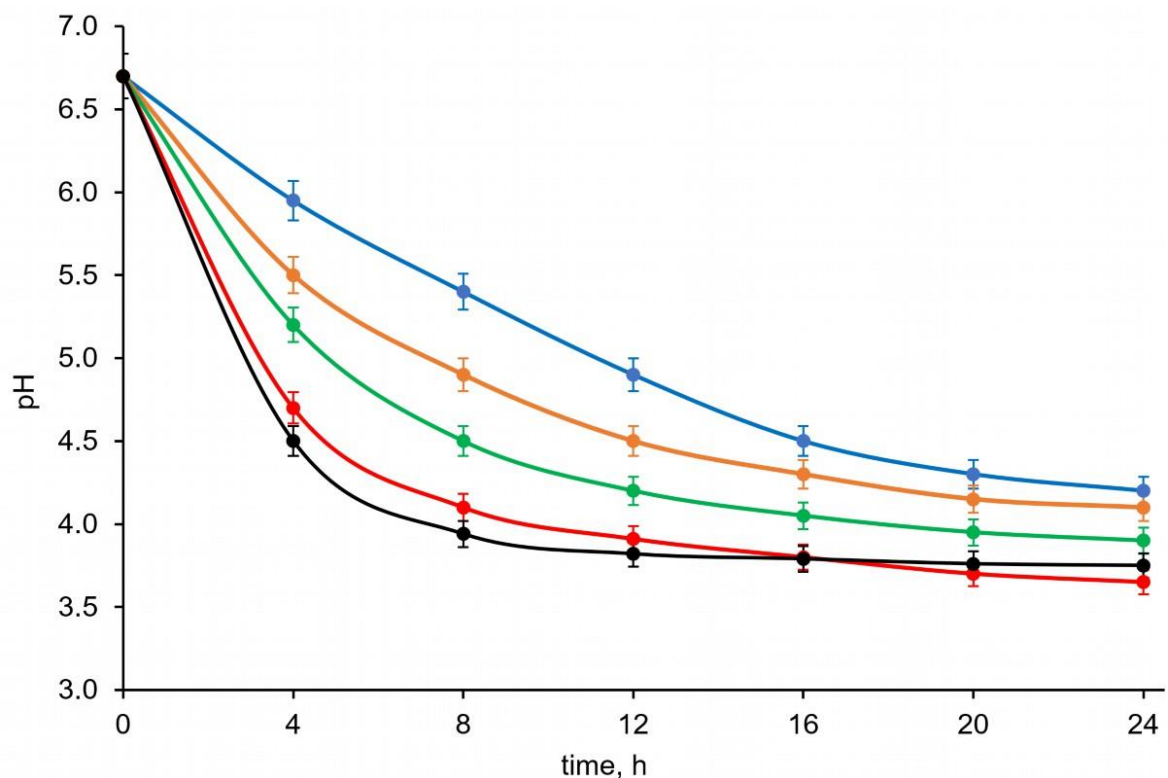


Figure 4. Effect of initial kefir grain concentration on kefir grain biomass propagation: decrease of pH value (2 % blue, 4 % orange, 6 % green, 8 % red, and 10 % black).

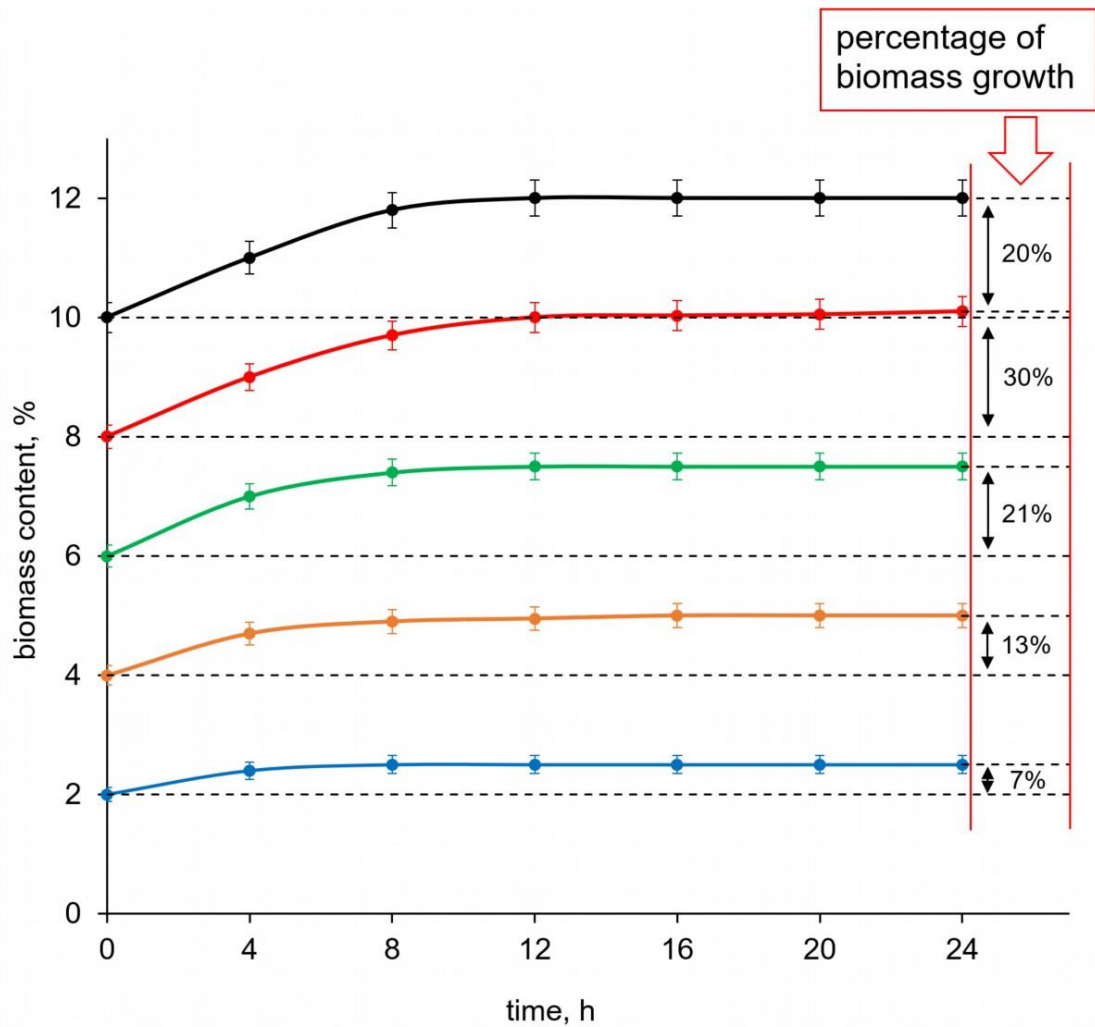


Figure 5. Effect of initial kefir grain concentration on kefir grain biomass propagation: biomass increment (2 % blue, 4 % orange, 6 % green, 8 % red, and 10 % black).

At the second stage of the experiment, we optimized the concentration of the studied additive samples 1–30. We used different concentrations 1–30: 0.1, 0.2, 0.3, 0.5, and 1.0 g/L. The obtained experimental data showed that the optimal concentration for all types of the tested samples is 0.2 g/L. This optimal concentration of any of 1–30 provides (i) the maximum increase in biomass and (ii) the minimum pH value after 12 and 24 hours after the start of the experiment.

Moreover, we found that within each series of samples **1–30**, the molecular weight of the chitosan does not have any noticeable effect on the studied biological activity. Thus, to simplify further experiments, we decided to use only systems based on moderate molecular weight chitosan (200 kDa, *i.e.* CS₂₀₀).

The third stage of the experiment was focused on a detailed study of the effect of **1–30** on kefir grain biomass propagation followed by identification of the leading system. Moreover, we compared the biological effects of **1–30** with those of the starting chitosan and the pure starting copper(II) salts *i.e.* CuSO₄ and Cu(CH₃COO)₂. The obtained results are summarized in **Figures 6 and 7**. The abilities of any of the tested systems **1–30** to cause the acidification of the kefir liquid pH and to mediate the increase in biomass are symbiotic. Thus, the system that promotes kefir grain biomass propagation to a greater extent (**Figure 6**) naturally results and in the greatest rate of acidification of the kefir liquid (**Figure 7**). In the paragraphs that follow, we discuss in detail the biological effects of **1–30** and attempt to explain the observed effects by structural features of the systems under test.

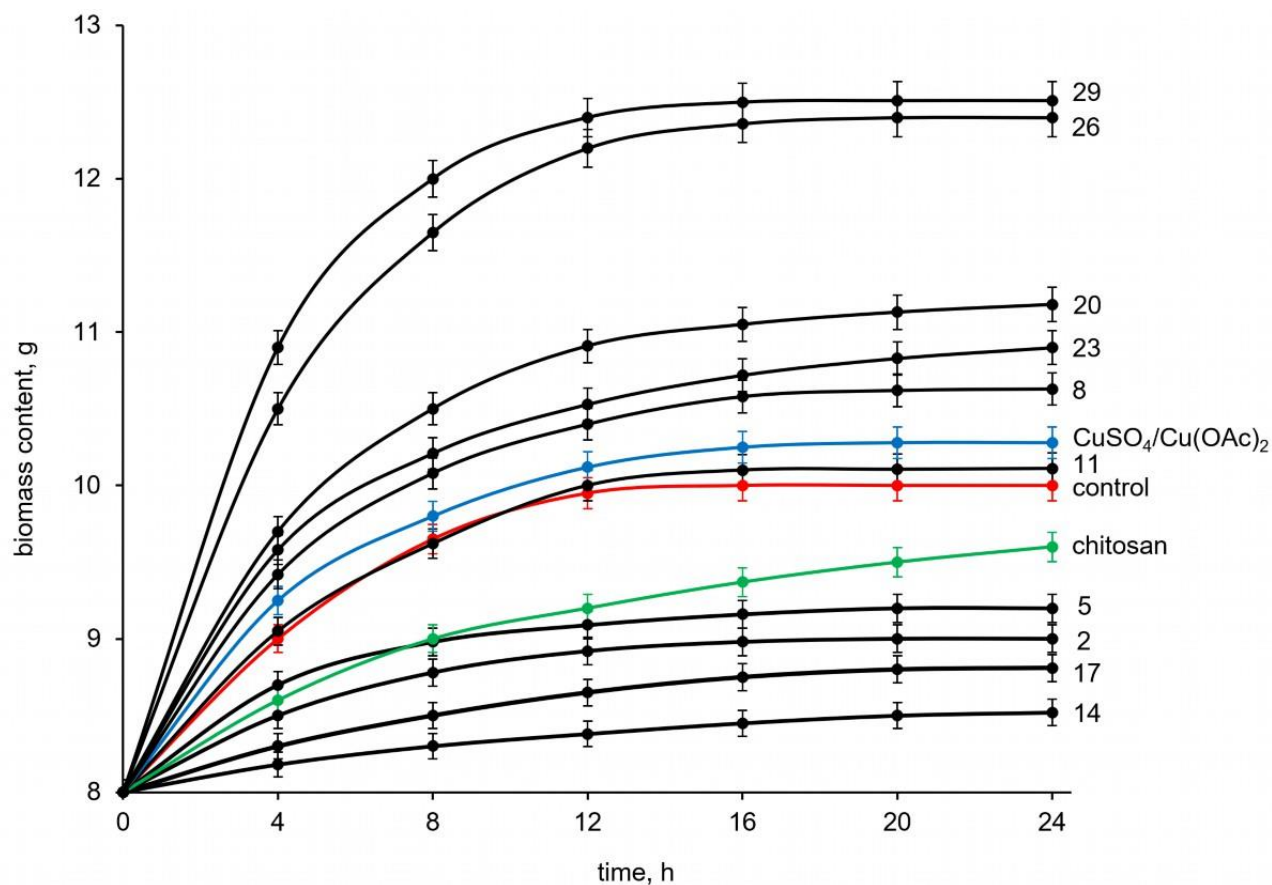


Figure 6. Comparison of the effect of the studied samples on the increase in the biomass of kefir grains.

First, samples **29** and **26** stimulate the growth of kefir grain biomass significantly more than all the others. Perhaps this is due to the absence of crystalline copper(II) salts *i.e.* CuSO₄ and Cu(CH₃COO)₂ in their composition (high *in vitro* toxicity of crystalline copper(II) salts CuSO₄ and Cu(CH₃COO)₂ will be shown in a later section).

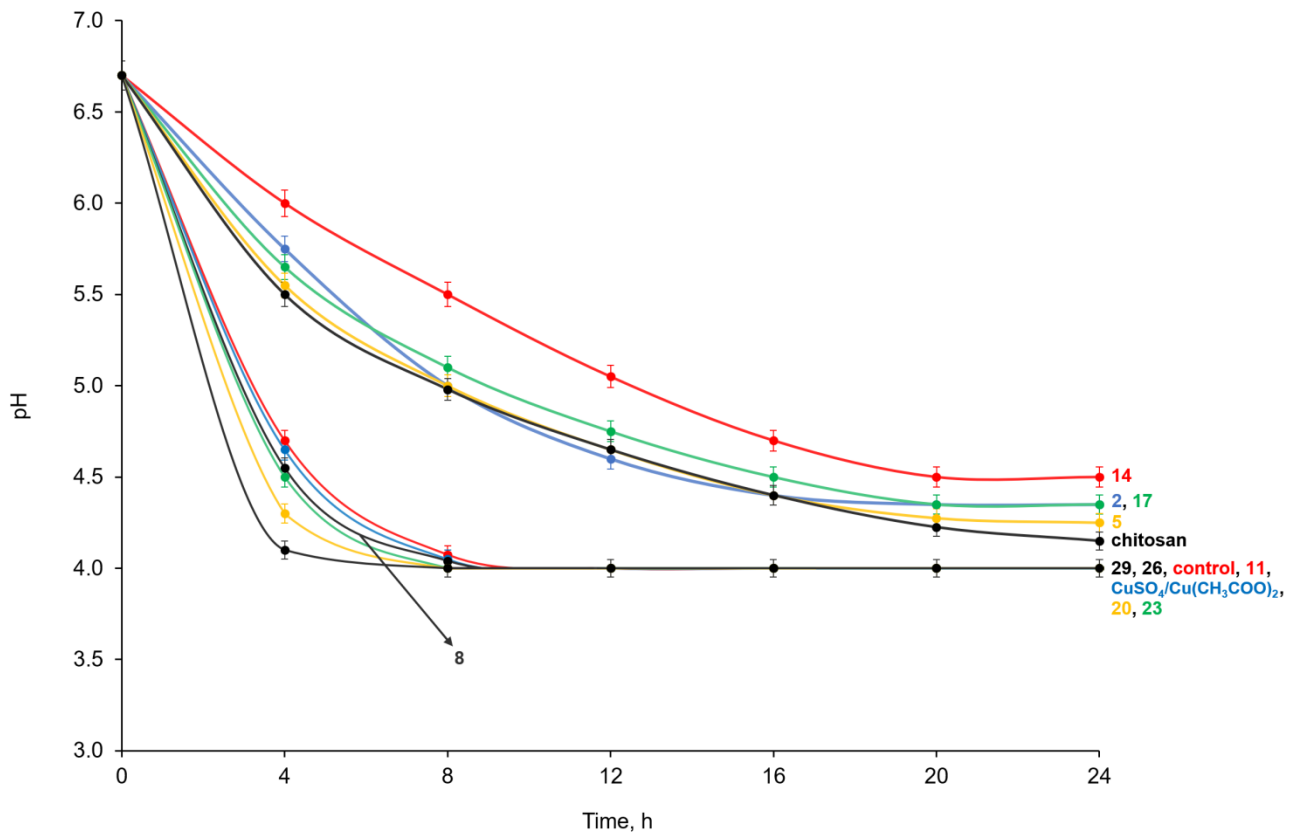


Figure 7. Comparison of the effect of the studied samples on the acidification of kefir liquid.

Sample **2** impairs kefir grain biomass growth compared to the control. This can be explained by its high positive zeta potential. As a rule, particles with a high positive zeta potential are the most toxic to living cells, including microbial cells (Chandrasekaran et al., 2020; Kritchenkov et al., 2012). Sample **5** is characterized by the same effect, but somewhat less pronounced. Perhaps this is because **5** has the form of a powder, while **2** has the form of nanoparticles. Usually, nanoparticles are characterized by more pronounced biological effects (Kritchenkov et al., 2020a; Kritchenkov et al., 2019a).

Samples **8** and **11**, on the contrary, contribute to the increase in the biomass of kefir grains. This may be due to the lower charge of particles **8** and **11** since they are covered with a layer of sodium hyaluronate polyanion. At the same time, a significantly greater biological effect of **8** may be due to its state in the form of nanoparticles.

The introduction of cholesterol into the system (samples **14** and **17**) leads to a significant inhibition of biomass growth in comparison with the control, which is due to the high toxicity of cholesterol-containing samples (see next section). As in previous cases, the biological activity of nanoparticles (**14**) was significantly higher than that of the powder-form (**17**).

Succination of the samples leads to a significant decrease in their zeta potential to negative values. This, in turn, results in a dramatic enhancement of kefir grain biomass growth by **20** and **23**. Succinated samples **26** and **29** have the most pronounced ability to increase kefir grain biomass growth, combined with the lowest toxicity (see next section). Thus, these systems were recognized as undoubted leaders, and the strategy of coating of chitosan-copper(II) particles with sodium hyaluronate followed by succination proved to be the most successful for elaboration of highly active systems based on chitosan and Cu^{2+} ions. In systems **26** and **29**, the nature of the anion (SO_4^{2-} or OAc^-) does not dramatically affect their biological activity, although we acknowledge that the system containing the acetate ion (**29**) is slightly more efficient.

Also, we would like to remark that species containing copper(II) only in the coordinated state (**25–30**) are significantly more active than those that additionally contain crystalline copper(II) salt, acetate or sulfate (**1–24**).

The question quite naturally arises whether composites **1–24** are capable of releasing copper ions Cu^{2+} into the kefir liquid, that is, being subject to leaching. To shed light on this point, at the end of the kefir experiments, the kefir liquid were subjected to centrifugation and filtration, followed by ICP analysis for the presence of Cu^{2+} ions. The ICP analysis demonstrated that composites containing copper(II) only in the coordinated state (**25–30**) do not release any copper species, while those that additionally contain crystalline copper(II) salt (**1–24**) are subject to leaching with release of copper. These results indicate that **25–30** can be considered safe for the food industry.

3.2.2. Toxicity studies

To assess the *in vitro* toxicity of the obtained samples **1–30**, we used the classical MTT test on a cultured HEK-293 cell line. The MTT test is a very convenient colorimetric test for evaluating the metabolic activity of cells. Only living cells are characterized by the ability to reduce 3-(4,5-dimethylthiazol-2-yl)-2,5-diphenyl-tetrazolium bromide to a compound called formazan, which has a purple color (Van Meerloo et al., 2011). Thus, the intensity of violet staining is directly proportional to the number of living cells. The experimental results of the MTT test are shown in **Table 1**.

Among the non-succinated species, the most toxic are cholesterol-containing samples **13–18**. The fact can be explained by their hydrophobic nature which determines their increased interaction with cell membranes. This, in turn, results in membrane disruption followed by cell death. The simplest samples **1–6** are characterized by different toxicity: **1–3** are more toxic than **4–6**. This more pronounced biological effect of **1–3** is probably due to their existence in nano form. Covering of **1–6** by sodium hyaluronate layer naturally decreases positive charge of the resultant particles **7–12** furnishing decrease of their toxicity.

Among succinated samples, **22–30** are practically non-toxic, their *in vitro* toxicity within margin of error does not differ from that of chitosan which is referred to non-toxic biopolymers (Kritchenkov et al., 2019b).

Thus, the succination that leads to recharge of the starting particles to negative charge values, proved to be an efficient strategy to achieve non-toxicity of the elaborated Cu(II)-based systems.

In the section 3.2.1, we found that among elaborated systems **1–30**, **26** and **29** are leaders regarding the stimulation of the kefir grain growth. Kefir is a food product and, therefore, like any food, it enters the gastrointestinal tract. Kefir drinks prepared using **26** or **29** inevitably contains

these supplements. Hence, in the frames of food safety regulations, the *in vivo* oral toxicity studies are needed to quantify the toxic risks caused by **26** or **29**.

We evaluated the *in vivo* subacute and acute toxicity of **26** and **29** in rats. Both acute and subacute tests lasted for 14 days. In the acute test, the animals were orally administrated by **26** or **29** only one time (at the 1st day of the experiment). Opposite, in the subacute test, the rates were administrated by the studied **26** or **29** daily for all 14 days. During 14 days of both acute and subacute tests, we controlled hematological and biochemical blood parameters of the animals (**Tables 2** and **3**). Moreover, after the tests, the status of the internal organs of experimental animals after autopsy was also assessed (**Table 4**).

The experimental data demonstrate that at a concentration of 2g per kg did not provoke nor acute poisoning symptoms of the rats neither the death of animals. The behavior of the treated rats did not differ from that of the control group of animals. During both acute and subacute tests, all reactions of the observed animals was within normal range. Coordination of movements, heart rate, respiratory rate and depth, water and food intake, urination frequency, urine color, defecation frequency and consistency of fecal masses, all of the above corresponded to the physiological norm in all observed animals during all test period. Hematological and biochemical parameters of the animals' blood (**Tables 2** and **3**) showed no difference between the control group and the treated group of rats. The autopsy after the tests did not reveal any toxic or other damage to the internal organs (**Table 4**). Based on these data, we concluded that that LD₅₀ > 2000 mg/kg. Thus, the studied samples **26** and **29** refer to the IV class of hazard (low-toxic substances).

Table 2. Hematological parameters of rats following oral administration of **26** and **29**.

| Hematological parameters | Acute test | | Subacute test | |
|--------------------------|------------|-----------------------|---------------|-----------------------|
| | Control | 26/29 | Control | 26/29 |
| <i>Male rats</i> | | | | |
| MCV (fL) | 67.31±3.45 | 66.99±3.43/66.72±3.41 | 64.98±1.41 | 64.87±1.40/64.16±1.91 |
| MCH (pg) | 18.87±0.71 | 18.78±0.70/18.67±0.69 | 19.01±0.57 | 18.79±0.54/18.67±0.51 |
| MCHC (g/dL) | 28.23±0.78 | 28.12±0.74/27.89±0.70 | 29.22±0.27 | 29.15±0.26/29.16±0.26 |

| | | | | |
|--|------------------|-----------------------------------|------------------|-----------------------------------|
| RBC ($\times 10^6/\mu\text{L}$) | 9.09 \pm 0.34 | 9.07 \pm 0.31/9.01 \pm 0.29 | 8.35 \pm 0.67 | 8.32 \pm 0.65/8.29 \pm 0.63 |
| WBC ($\times 10^3/\mu\text{L}$) | 8.51 \pm 1.67 | 8.42 \pm 1.59/8.46 \pm 1.61 | 8.03 \pm 2.01 | 8.01 \pm 1.97/8.00 \pm 1.98 |
| Platelets ($\times 10^3/\mu\text{L}$) | 843.00 \pm 13 | 837.00 \pm 132.62/ 5.94 | 1207.00 \pm 19 | 1189.00 \pm 187.73/ 3.54 |
| Hct (%) | 63.01 \pm 3.96 | 62.96 \pm 3.87/62.91 \pm 3.81 | 53.74 \pm 3.53 | 53.04 \pm 3.48/53.45 \pm 3.51 |
| Hgb (g/dL) | 18.78 \pm 1.45 | 18.64 \pm 1.44/18.71 \pm 1.45 | 15.68 \pm 1.07 | 15.24 \pm 1.04/15.28 \pm 1.05 |
| <i>Female rats</i> | | | | |
| MCV (fL) | 64.36 \pm 3.26 | 64.07 \pm 3.25/63.89 \pm 3.24 | 61.04 \pm 1.26 | 60.94 \pm 1.24/60.87 \pm 1.23 |
| MCH (pg) | 18.13 \pm 0.69 | 17.95 \pm 0.67/18.02 \pm 0.68 | 18.59 \pm 0.49 | 18.45 \pm 0.47/18.44 \pm 0.46 |
| MCHC (g/dL) | 27.94 \pm 0.73 | 27.78 \pm 0.71/27.86 \pm 0.72 | 29.45 \pm 0.34 | 29.37 \pm 0.33/29.41 \pm 0.34 |
| RBC ($\times 10^6/\mu\text{L}$) | 9.01 \pm 0.33 | 8.97 \pm 0.30/8.95 \pm 0.30 | 9.11 \pm 0.56 | 9.07 \pm 0.55/9.10 \pm 0.56 |
| WBC ($\times 10^3/\mu\text{L}$) | 5.79 \pm 0.98 | 5.78 \pm 0.96/5.74 \pm 0.95 | 4.62 \pm 0.27 | 4.59 \pm 0.25/4.60 \pm 0.26 |
| Platelets ($\times 10^3/\mu\text{L}$) | 987.00 \pm 14 | 981.00 \pm 140.25/ 1.76 | 1099.00 \pm 20 | 1086.00 \pm 204.65/ 6.23 |
| Hct (%) | 58.08 \pm 3.71 | 57.87 \pm 3.67/57.67 \pm 3.64 | 55.97 \pm 3.73 | 55.81 \pm 3.71/55.72 \pm 3.70 |
| Hgb (g/dL) | 16.32 \pm 1.32 | 16.27 \pm 1.31/16.29 \pm 1.31 | 16.72 \pm 1.31 | 16.68 \pm 1.30/16.71 \pm 1.31 |
| Mean value \pm SD | | | | |

Table 3. Blood biochemical parameters of rats following oral administration of **26** and **29**.

| Blood biochemical parameters | Acute test | | Subacute test | |
|------------------------------------|------------------|-----------------------------------|-------------------|---|
| | Control | 26/29 | Control | 26/29 |
| <i>Male rats</i> | | | | |
| Albumin (g/dL) | 4.20 \pm 0.16 | 4.17 \pm 0.15/4.19 \pm 0.16 | 3.59 \pm 0.23 | 3.63 \pm 0.24/3.65 \pm 0.25 |
| AST (U/L) | 84.00 \pm 6.74 | 82.75 \pm 6.71/83.01 \pm 6.72 | 97.12 \pm 11.84 | 93.34 \pm 11.56/ 95.73 \pm 11.73 |
| ALT (U/L) | 11.70 \pm 5.78 | 11.50 \pm 5.76/11.47 \pm 5.75 | 27.09 \pm 6.27 | 26.86 \pm 6.19/26.71 \pm 6.14 |
| BUN (mg/dL) | 15.41 \pm 1.38 | 13.88 \pm 1.37/14.34 \pm 1.37 | 13.45 \pm 1.48 | 13.49 \pm 1.50/13.46 \pm 1.49 |
| Creatinine (mg/dL) | 0.35 \pm 0.05 | 0.29 \pm 0.05/0.31 \pm 0.05 | 0.34 \pm 0.05 | 0.33 \pm 0.05/0.33 \pm 0.05 |

| | | | | |
|----------------------------|--------------|-------------------------------|-------------|-----------------------|
| Glucose (mg/dL) | 209.75±31.46 | 191.50±30.96/ 187.35±29.56 | 79.12±10.87 | 93.48±12.48/87±11.47 |
| Total bilirubin (mg/dL) | 0.30±0.05 | 0.29±0.05/0.29±0.05 | 0.35±0.05 | 0.38±0.05/0.37±0.05 |
| Total protein (g/dL) | 6.32±0.31 | 6.32±0.31/6.31±0.31 | 6.16±0.27 | 6.21±0.28/6.23±0.29 |
| Female rats | | | | |
| Albumin (g/dL) | 4.60±0.19 | 4.67±0.20/4.61±0.19 | 4.41±0.31 | 4.34±0.30/4.39±0.31 |
| AST (U/L) | 66.75±6.24 | 67.46±6.27/66.91±6.25 | 79.25±6.87 | 79.00±6.82/78.94±6.81 |
| ALT (U/L) | 12.47±2.48 | 12.54±2.51/12.56±2.52 | 21.97±6.19 | 21.71±6.11/21.78±6.14 |
| BUN (mg/dL) | 14.01±1.51 | 14.13±1.52/14.02±1.51 | 16.72±1.15 | 15.98±1.03/15.99±1.04 |
| Creatinine (mg/dL) | 0.29±0.05 | 0.29±0.05/0.29±0.05 | 0.34±0.05 | 0.33±0.05/0.33±0.05 |
| Glucose (mg/dL) | 159.00±35.27 | 167.00±36.74/ 162.00±35.98 | 44.50±8.96 | 49.00±9.17/51.00±9.26 |
| Total bilirubin (mg/dL) | 0.44±0.05 | 0.45±0.05/0.44±0.05 | 0.53±0.06 | 0.49±0.06/0.51±0.06 |
| Total protein (g/dL) | 6.71±0.36 | 6.76±0.37/6.76±0.37 | 6.21±0.29 | 6.14±0.26/6.18±0.28 |
| Mean value ± SD | | | | |

Table 4. Relative organ weights of rats following oral administration of **26** and **29**.

| Relative organ weight (g/100 g of body weight) | Acute test | | Subacute test | |
|---|------------|-----------------------|---------------|---------------------|
| | Control | 26/29 | Control | 26/29 |
| Male rats | | | | |
| Heart | 0.75±0.07 | 0.79±0.08/0.82±0.09 | 0.23±0.02 | 0.24±0.02/0.23±0.02 |
| Kidney | 1.38±0.18 | 1.40±0.21/1.39±0.19 | 0.41±0.04 | 0.38±0.03/0.37±0.03 |
| Liver | 10.67±1.01 | 10.81±1.12/10.85±1.15 | 3.18±0.17 | 3.23±0.19/3.25±0.20 |
| Spleen | 2.41±0.19 | 2.43±0.20/2.44±0.21 | 0.83±0.02 | 0.87±0.03/0.84±0.02 |
| Female rats | | | | |
| Heart | 0.55±0.06 | 0.59±0.07/0.58±0.06 | 0.31±0.03 | 0.30±0.03/0.30±0.03 |

| | | | | |
|-----------------|-----------|---------------------|-----------|---------------------|
| Kidney | 0.91±0.13 | 0.92±0.14/0.93±0.15 | 0.45±0.04 | 0.44±0.05/0.43±0.05 |
| Liver | 6.34±0.51 | 6.37±0.53/6.41±0.56 | 3.09±0.27 | 3.14±0.24/3.12±0.25 |
| Spleen | 1.54±0.16 | 1.53±0.15/1.52±0.15 | 0.68±0.05 | 0.69±0.06/0.70±0.06 |
| Mean value ± SD | | | | |

4. Conclusion

The results of this work can be considered in the following main perspectives.

Firstly, we elaborated new chitosan-based Cu(II)-containing composites of several types: (i) the simplest Cu²⁺/chitosan blended composites, (ii) the hyaluronate-covered, (iii) cholesterol containing, (iv) the simplest succinated, and (v) the hyaluronate-covered succinated ones. The elaborated composites are presented in two forms, *i.e.* conventional powder and nanoparticles. In the composites, Cu²⁺ ions can exist in fully coordinated to chitosan state or a part of Cu²⁺ can be crystallized as a copper(II) salt.

Secondly, we found that the pure Cu²⁺ salts (acetate and sulfate) enhance kefir biomass growth, while the pure chitosan it inhibits. Blending of Cu²⁺ and succinated chitosan or succinated chitosan covered by hyaluronate stimulates kefir grain propagation. This stimulation reaches its dramatical apogee in the case of succinated hyaluronate covered Cu²⁺/chitosan composites, which are undoubted leaders. Thus, the fact is explained by symbiotic effect of Cu²⁺ ions and polymeric matrices. The authors are aware that further experiments are needed to study the possibility of scaling both the synthesis processes of these composites and the processes of stimulating the growth of microorganisms.

Thirdly, we evaluated the *in vitro* toxicity of the elaborated composites and found that incorporation of Cu²⁺ in polymeric matrix dramatically decreases the toxic effect of copper ions toward to living cells. The leading composites **26** and **29** also demonstrated low *in vivo* acute and subacute toxicity which allowed us to refer them to the IV class of hazard (low-toxic substances). Of course, we presented only primary experiments describing the low toxicity of the resulting

composites. For further detailed assessment, histological, morphological and other studies are necessary.

Finally, the obtained results are interesting from a biotechnological point of view for development of protocols for quick and convenient preparation of kefir drinks, and this project is underway in our group.

Acknowledgements

This paper has been supported by the RUDN University Strategic Academic Leadership Program (recipient: A.A. Kirichuk, award no. 202713-0-000 “Development of a scientifically based methodology for the ecological adaptation of foreign students to new environmental conditions”).

References

- Bashir, S., et al. (2015). N-succinyl chitosan preparation, characterization, properties and biomedical applications: a state of the art review, *Reviews in Chemical Engineering*. 31(6), 563-597.
- Cammarata, C. R., et al. (2015). Carbodiimide Induced Cross-Linking, Ligand Addition, and Degradation in Gelatin, *Molecular Pharmaceutics*. 12(3), 783-793.
- Chandrasekaran, M., et al. (2020). Antibacterial Activity of Chitosan Nanoparticles: A Review, *Processes*. 8(9).
- Farooq, T., et al. (2022). Priming with copper-chitosan nanoparticles elicit tolerance against PEG-induced hyperosmotic stress and salinity in wheat, *BMC Chemistry*. 16(1), 23.
- Gandra, J. R., et al. (2018). Soybean whole-plant ensiled with chitosan and lactic acid bacteria: Microorganism counts, fermentative profile, and total losses, *Journal of Dairy Science*. 101(9), 7871-7880.
- Goy, R. C., et al. (2009). A review of the antimicrobial activity of chitosan, *Polimeros*. 19(3), 241-247.
- Han, X., et al. (2012). Effects of copper on the post acidification of fermented milk by *St. thermophilus*, *J Food Sci*. 77(1), M25-8.
- Hosseinnejad, M., Jafari, S. M. (2016). Evaluation of different factors affecting antimicrobial properties of chitosan, *International Journal of Biological Macromolecules*. 85, 467-475.
- Kritchenkov, A. S., et al. (2012). A palladium(II) center activates nitrile ligands toward 1,3-dipolar cycloaddition of nitrones substantially more than the corresponding platinum(II) center, *Inorganic Chemistry*. 51(21), 11971-9.
- Kritchenkov, A. S., et al. (2020a). Novel heterocyclic chitosan derivatives and their derived nanoparticles: Catalytic and antibacterial properties, *International Journal of Biological Macromolecules*. 149, 682-692.
- Kritchenkov, A. S., et al. (2019a). Ultrasound-assisted Cu(I)-catalyzed azide-alkyne click cycloaddition as polymer-analogous transformation in chitosan chemistry. *High*

- antibacterial and transfection activity of novel triazol betaine chitosan derivatives and their nanoparticles, *International Journal of Biological Macromolecules*. 137, 592-603.
- Kritchenkov, A. S., et al. (2019b). Ultrasound-assisted catalyst-free phenol-yne reaction for the synthesis of new water-soluble chitosan derivatives and their nanoparticles with enhanced antibacterial properties, *International Journal of Biological Macromolecules*. 139, 103-113.
- Kritchenkov, A. S., et al. (2020b). Active antibacterial food coatings based on blends of succinyl chitosan and triazole betaine chitosan derivatives, *Food Packaging and Shelf Life*. 25, 100534.
- Kritchenkov, A. S., et al. (2013). Selective Nucleophilic Oxygenation of Palladium-Bound Isocyanide Ligands: Route to Imine Complexes That Serve as Efficient Catalysts for Copper-/Phosphine-Free Sonogashira Reactions, *Organometallics*. 32(6), 1979-1987.
- Kritchenkov, A. S., et al. (2020c). Chitosan derivatives and their based nanoparticles: ultrasonic approach to the synthesis, antimicrobial and transfection properties, *Carbohydrate Polymers*. 242, 116478.
- Lari, R. B., et al. (2011). Sorption behavior of Zn (II) ions by low cost and biological natural hydroxyapatite/chitosan composite from industrial waste water, *Journal of Food, Agriculture and Environment*. 9(3&4), 892-897.
- Liu, L., et al. (2018). Prebiotic-Like Effects of Water Soluble Chitosan on the Intestinal Microflora in Mice, *International Journal of Food Engineering*. 14(7-8).
- Mallik, A. K., et al. (2020) Chapter 6 - Chitin nanomaterials: preparation and surface modifications, In *Handbook of Chitin and Chitosan* (S. Gopi, et al., Ed.)^Eds.) ed., p^pp 165-194, Elsevier.
- Mekahlia, S., Bouzid, B. (2009). Chitosan-Copper (II) complex as antibacterial agent: synthesis, characterization and coordinating bond- activity correlation study, *Physics Procedia*. 2(3), 1045-1053.
- Pooladi, A., Bazargan-Lari, R. (2023). Adsorption of zinc and copper ions simultaneously on a low-cost natural chitosan/hydroxyapatite/snail shell/nano-magnetite composite, *Cellulose*. 30(9), 5687-5705.
- Qian, Z., et al. (2022). Injectable self-healing polysaccharide hydrogel loading CuS and pH-responsive DOX@ZIF-8 nanoparticles for synergistic photothermal-photodynamic-chemotherapy of cancer, *Journal of Materials Science & Technology*. 127, 245-255.
- Qin, Y., et al. (2020). Cationic chitosan derivatives as potential antifungals: A review of structural optimization and applications, *Carbohydrate Polymers*. 236, 116002.
- Sahariah, P., Másson, M. (2017). Antimicrobial Chitosan and Chitosan Derivatives: A Review of the Structure–Activity Relationship, *Biomacromolecules*. 18(11), 3846-3868.
- Sahm, D. H. (1991) Antibacterial susceptibility tests: dilution methods, In *Manual of clinical microbiology* (P. R. Murray, Ed.)^Eds.) ed., p^pp 1105-1116, ASM Press, Washington, D.C.
- Shih, P. Y., et al. (2019). A Potential Antifungal Effect of Chitosan Against *Candida albicans* Is Mediated via the Inhibition of SAGA Complex Component Expression and the Subsequent Alteration of Cell Surface Integrity, *Front Microbiol*. 10, 602.
- Skorik, Y. A., et al. (2017). Synthesis of N-succinyl- and N-glutaryl-chitosan derivatives and their antioxidant, antiplatelet, and anticoagulant activity, *Carbohydrate Polymers*. 166, 166-172.
- Tang, X., et al. (2022). Graphene oxide/chitosan/potassium copper hexacyanoferrate(II) composite aerogel for efficient removal of cesium, *Chemical Engineering Journal*. 444, 136397.
- Van Meerloo, J., et al. (2011). Cell sensitivity assays: The MTT assay, *Methods in Molecular Biology*. 731, 237-245.
- Varlamov, V. P., et al. (2020). Chitin/Chitosan and Its Derivatives: Fundamental Problems and Practical Approaches, *Biochemistry-Moscow*. 85(SUPPL 1), 154-176.
- Williams, A., Ibrahim, I. T. (1981). Carbodiimide chemistry: recent advances, *Chemical Reviews*. 81(6), 589-636.

- Yanat, M., Schroën, K. (2021). Preparation methods and applications of chitosan nanoparticles; with an outlook toward reinforcement of biodegradable packaging, *Reactive and Functional Polymers*. 161, 104849.
- Zhao, C., et al. (2022). Bioceramic-based scaffolds with antibacterial function for bone tissue engineering: A review, *Bioactive Materials*. 18, 383-398.